RSC Advances

PAPER

View Article Online
View Journal | View Issue

Cite this: *RSC Adv.*, 2017, **7**, 45807

New D–π–A dyes incorporating dithieno[3,2-*b*:2′,3′-*d*]pyrrole (DTP)-based π-spacers for efficient dye-sensitized solar cells†

Jingwen Jia, Yu Chen,* Liangsheng Duan, Zhe Sun, Mao Liang and Song Xue*

Received 14th August 2017
Accepted 21st September 2017

DOI: 10.1039/c7ra08965a

rsc.li/rsc-advances

Three D–π–A sensitizers incorporating dithieno[3,2-*b*:2′,3′-*d*]pyrrole (DTP)-based π-linkers were synthesized for fabricating efficient dye-sensitized solar cells (DSSCs). The DTP-based π-spacers were attached by 10-phenyl-10*H*-phenothiazine (**JW1**), 5,5,10,10,15,15-hexapropyl-10,15-dihydro-5*H*-diindeno[1,2-*a*:1′,2′-*c*]fluorene (**JW2**) and 4-hexyloxyphenyl (**JW3**). The bulky groups and alkyl chains are introduced to suppress dye aggregation as well as reduce electron recombination. An additional double bond spacer was introduced between the arylamine donor and DTP-based π-spacer in the studied dyes. Based on the theoretical calculation results, all of the dye molecules display good electron transport. The photovoltaic performances of device based on **JW1**, **JW2** and **JW3** were measured by *J*–*V* characterizations in Co-phen based electrolyte, achieving power conversion efficiencies of 7.09%, 7.87% and 6.50%, respectively. The incident photon-to-current conversion efficiency (IPCE) follows the order **JW2** > **JW1** > **JW3**, which is accordance with their photovoltaic performances. IMVS results indicate that the three dyes incorporating the modified DTP-based π-spacers have an influence on the CB shift of TiO_2 and the inhibition of charge recombination. Therefore, the DTP-based π-spacer is a promising building block for developing new dyes to build highly efficient DSSCs.

1. Introduction

Dye-sensitized solar cells (DSSCs) have drawn much attention since the work of O'Regan and Grätzel in 1991.[1,2] DSSCs can reduce the production cost and exhibit good photovoltaic performances so as to become a good substitute for expensive silicon solar cells. To date, various sensitizers have been used to fabricate highly efficient DSSCs, involving metal complex dyes[3–8] and metal-free organic dyes.[9–14] Metal-free organic dyes are amenable to structure modification and easy to purify. The power conversion efficiency (PCE) of DSSCs based on metal-free organic dyes has been greatly improved by structure design. Kakiage and co-workers reported that DSSCs co-sensitized by ADKEA-1 and LEG-4 exhibited a highest PCE of over 14%.[15–17] Recently, it has been demonstrated by Freitag and co-workers that a DSSC achieved a very high PCE of 28.9% under ambient light conditions, using two organic sensitizers coded D35 and XY1.[18] Therefore, metal-free organic dyes show promising advantages in fabricating highly effective DSSCs.

The design of metal-free organic dyes can focus on molecular engineering of the electron donor, π-spacer, and acceptor for good light response, large anchoring amount and suitable energy levels.[19–21] Suitable molecular energy levels of organic dyes to match electrolyte are beneficial to achieve an efficient regeneration of the oxidized dyes.[22] Triarylamines are mostly used as effective electron donor groups in the sensitizer molecules, which can be feasibly synthesized and modified. Cyanoacetic acid is widely used as end groups with good electron accepting ability. The π-spacers of the organic dyes have a great influence on electron transfer between donors and acceptors in a dye molecule. In recent years, π-conjugated spacers containing thiophene rings have been reported showing positive effects on improving photovoltaic performances of organic sensitizers, such as thieno[3,2-*b*]thiophene,[23] cyclopenta[1,2-*b*:5,4-*b*′]dithiophene[24–26] and dithieno[3,2-*b*:2′,3′-*d*]pyrrole (DTP).[27–29]

DTP is accessible with a yield in one step up to 80%, and the N-position provides great opportunity for the control of dye aggregation, which makes it good for DSSC applications. As reported in our previous study,[30] DTP can be easily modified by the introduction of long-chain alkyl groups on the bridging nitrogen, and DSSCs fabricated by these DTP-based dyes achieved a PCE of 8.14%. Wang and co-workers reported a series of arylamine organic dyes bearing *N*-heterocycle-substituted DTP spacers displayed a PCE of 8.20%.[31] Polander and co-workers synthesized two donor–π-spacer–acceptor (D–π–A) dyes based on the DTP π-

Tianjin Key Laboratory of Organic Solar Cells and Photochemical Conversion, School of Chemistry & Chemical Engineering, Tianjin University of Technology, Tianjin 300384, China. E-mail: cytjut@163.com; xuesong@ustc.edu.cn; Fax: +86-22-60214252

† Electronic supplementary information (ESI) available. See DOI: 10.1039/c7ra08965a

bridge and compared with their cyclopenta[1,2-*b*:5,4-*b*′]dithiophene (CPDT) analogues.[32] Based on their results, DTP-based device exhibited an increased open circuit photovoltage values and improved charge-transfer kinetics relative to the CPDT systems. The present researches suggest DTP has a great potential for the design of efficient metal-free organic sensitizers in the field of DSSCs. The effects of *N*-substituents on dyes properties and device performances are worthy to explore.

In this work, three new D–π–A metal-free organic dyes were developed for DSSC application (**JW1**, **JW2** and **JW3**). **JW1** and **JW2** have been synthesized by introducing bulky groups of 10-phenyl-10*H*-phenothiazine and 5,5,10,10,15,15-hexapropyl-10,15-dihydro-5*H*-diindeno[1,2-*a*:1′,2′-*c*]fluorene (truxene) onto the N-position of DTP spacers, respectively. **JW3** was prepared by incorporating 4-hexyloxyphenyl as a reference compound. In the three dyes, the triphenylamine substituted by hexyloxy groups were used as electron donating group, and 2-cyanoacrylic acid was used as electron accepting group. A double bond was inserted between triphenylamine donor and DTP spacer, aiming to enhance π-conjugation length of dye molecules.[33] The UV-vis absorption, optimized geometrical and electronic structures by density functional theory (DFT) calculations, and cyclic voltammetry behaviors of the three D–π–A dyes were characterized. DSSCs based on **JW1**, **JW2** and **JW3** were fabricated by using Co-phen based (phen = 1,10-phenanthroline) electrolytes with 4-*tert*-butylpyridine (TBP). The photovoltaic performances of DSSCs based on the studied dyes are measured by *J*–*V* characteristics, and the corresponding incident photon-to-current conversion efficiency (IPCE) spectra of **JW1**, **JW2** and **JW3** were recorded. The results show **JW1** and **JW2** bearing bulky groups exhibit a more positive influence on enhancing efficiency of DSSCs than **JW3**. The dyes effect on device performance was further discussed by conducting the measurements of the controlled intensity modulated photovoltage spectroscopy (IMVS).

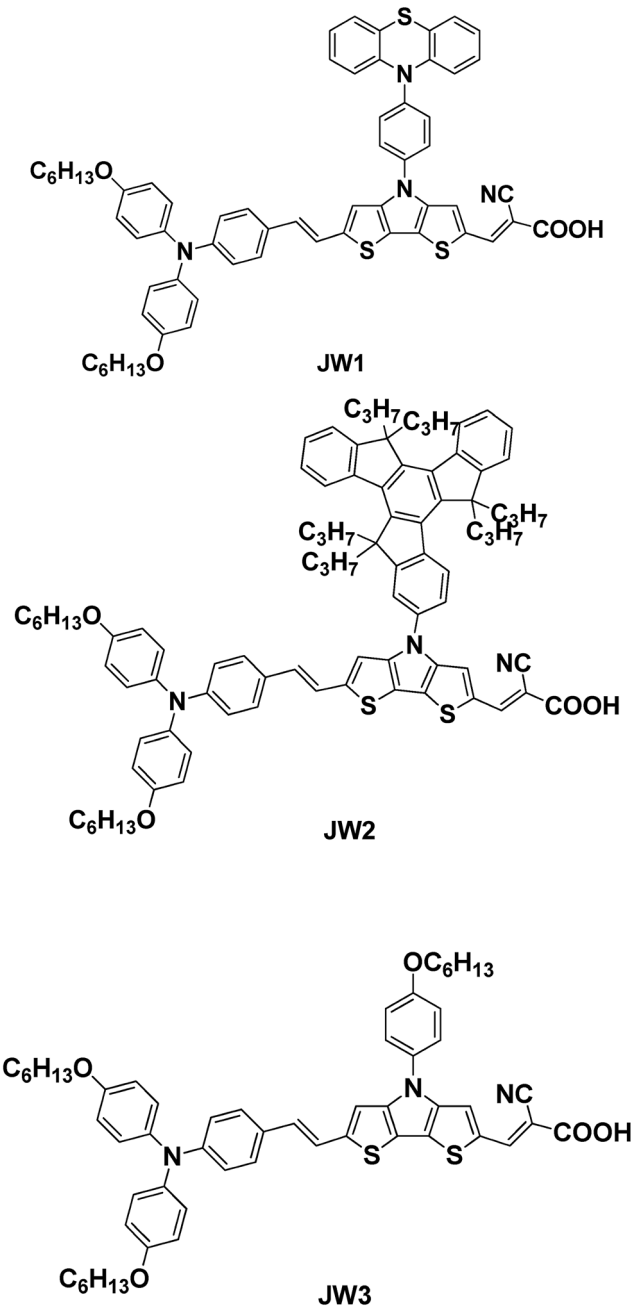

Fig. 1 Chemical structures of JW1, JW2 and JW3.

2. Experimental

2.1. Instrument and materials

The chemical structures of target products **JW1**, **JW2** and **JW3** are shown in Fig. 1. BINAP, P(*t*-Bu)$_3$, *t*-BuONa, $Pd_2(dba)_3$ and $PPh_3 \cdot HBr$ were purchased from J&K Chemical. Cyanoacetic acid was purchased from Energy Chemical (China). The solvents and chemicals used in this work were analytical grade and purchased from Energy Chemical (China). The reagents for reactions and spectral measurements were dried and distilled before use. The treatment on solvents and reactants is shown in ESI.†

^{1}H NMR and ^{13}C NMR spectra were recorded on a Bruker AM-400 spectrometer. The reported chemical shifts were against TMS. High resolution mass spectra were obtained with a Micromass GCT-TOF mass spectrometer. The melting point was taken on a RY-1 thermometer and the temperatures were uncorrected.

2.2. Photophysical properties and electrochemical properties

The absorption spectra of dyes and sensitized films were measured by SHIMADZU UV-2600 spectrophotometer. Fluorescence measurements were carried out with a HITACHI F-4500 fluorescence Spectrophotometer.

Cyclic voltammetry (CV) measurements for sensitized films were measured by a Zennium electrochemical workstation (ZAHNER, Germany), with sensitized electrodes as the working electrode, Pt-wires as the counter electrode, and an Ag/AgCl electrode as the reference electrode at a scan rate of 25 mV s^{-1}. Tetrabutylammonium perchlorate (TBAP, 0.1 M) and acetonitrile were used as supporting electrolyte and solvent, respectively. Ferrocene was used as standard in the measurements.

Charge densities at open circuit and intensity modulated photovoltage spectroscopy (IMVS) were performed on a Zennium

electrochemical workstation (ZAHNER, Germany), which includes a green light emitting diode (LED, 525 nm) and the corresponding control system. Charge densities and IMVS were measured on a two electrode system with the TiO_2-photoanode as a working electrode and the photocathode as the counter/reference electrodes. The intensity-modulated spectra were measured at room temperature with light intensity ranging from 5 to 75 W m^{-2}, in modulation frequency ranging from 0.1 Hz to 10 kHz, and with modulation amplitude less than 5% of the light intensity.

2.3. The DSSCs fabrication and characterization

A TiO_2 electrode (0.156 cm^2) was developed on a precleaned fluorine-doped tin oxide (FTO) conducting glass (Nippon Sheet Glass, Hyogo, Japan, sheet resistance of 14 Ω sq^{-1}), and the detailed fabrication procedure was included in ESI.† The dye was loaded by immersing it into a 300 μM dye solution (ethanol/CH_2Cl_2 = 2/3, v/v) for 12 h at room temperature. Then washed the dye coated titania electrode with dry ethanol. The pre-washed FTO glass was deposited with Pt catalyst by coating with H_2PtCl_6 solution (40 mM in ethanol), and used the heat treatment sinter at 395 °C for 15 min to get photocathode. The sensitized electrode and Pt-counter electrode were assembled into a sandwich type cell by a 25 mm-thick Surlyn (DuPont) hot-melt gasket and sealed up by heating. The Co-phen electrolyte is composed of 0.25 M [Co(II) $(phen)_3](PF_6)_2$, 0.05 M [Co(III) $(phen)_3](PF_6)_3$, 0.5 M TBP and 0.1 M LiTFSI in acetonitrile.

The photocurrentevoltage (*J–V*) characteristics of the solar cells based on the studied dyes were carried out using a Keithley 2400 digital source meter controlled by a computer and a standard AM1.5 solar simulator-Oriel 91160-1000 (300 W) SOLAR SIMULATOR 2 × 2 BEAM. The light intensity was calibrated by an Oriel reference solar cell. The action spectra of monochromatic incident photon-to-current conversion efficiency (IPCE) for solar cell were performed by using a commercial setup (QTest Station 2000 IPCE Measurement System, CROWNTECH, USA).

2.4. Synthesis

The synthesis route for **JW1**, **JW2** and **JW3** are shown in Scheme 1. The intermediates of compounds **1–5** have been reported in literatures.[34–36] The ^1H NMR and ^{13}C NMR data of **7a–c**, **8a–c**, **JW1**, **JW2** and **JW3** are listed in ESI.†

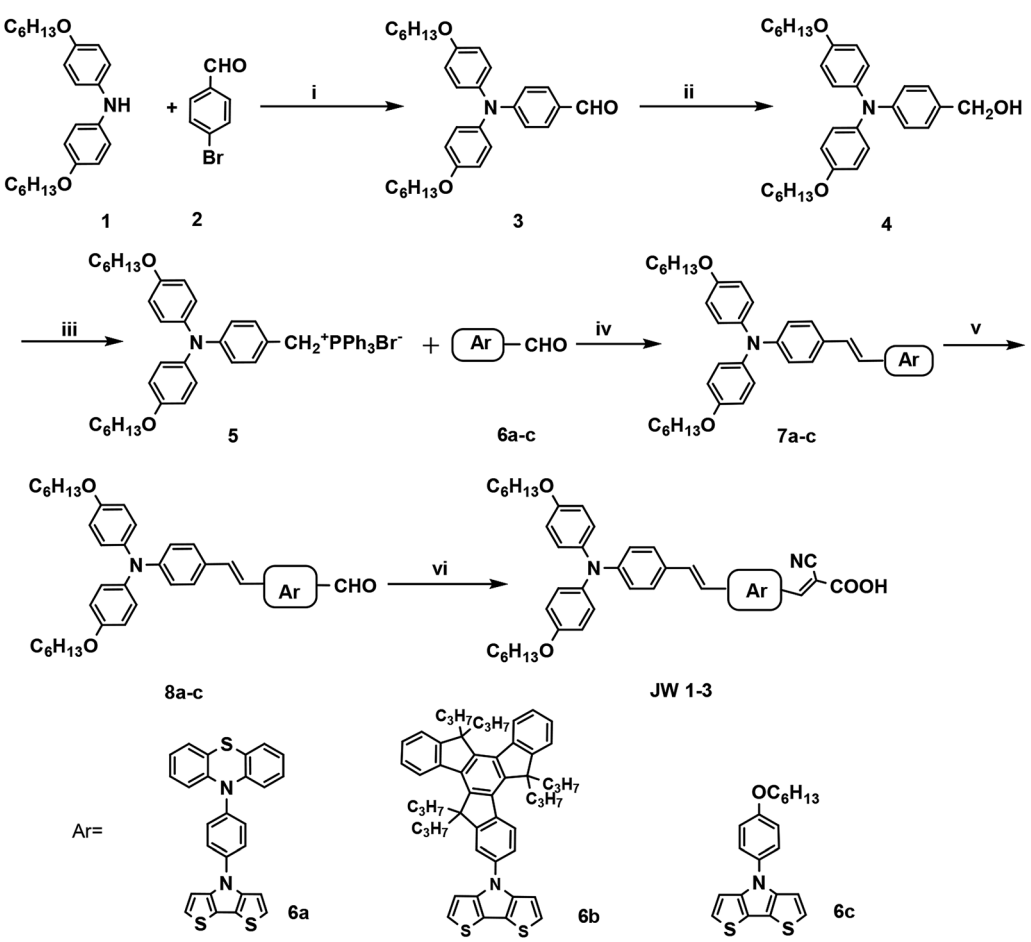

Scheme 1 The synthesis route of **JW1**, **JW2** and **JW3**. Conditions: (i) *t*-BuONa, $Pd_2(dba)_3$, P(*t*-Bu)$_3$, toluene, N_2, reflux, 14 h; (ii) $NaBH_4$, EtOH, N_2, RT, 4 h; (iii) $PPh_3 \cdot HBr$, $CHCl_3$, reflux, 4 h; (iv) *t*-BuOK, THF, RT, 24 h; (v) OCl_3, DMF, DEC, 0 °C then reflux, 8 h; (vi) piperidine, cyano-acetic acid, $CHCl_3/CH_3CN$ (v/v, 1/2), reflux, 8 h.

2.4.1 General procedure for the synthesis of compounds 7a, 7b, 7c. To a 100 mL two-neck round-bottom flask, dissolved compound **5** (0.38 mmol, 317 mg) in anhydrous THF (10 mL). The system was purged with nitrogen several times. At 0 °C, the THF solution of *t*-BuOK (0.69 mmol, 71 mg) was added dropwise, and the solution became deep red. The system was kept at 0 °C. After 1 h, the THF solution of **6a–c** (0.345 mmol) was added slowly. The mixture was cooled to room temperature and stirred overnight. Water was added to pull the plug on the reaction and the product was extracted with dichloromethane. The combined organic layer was washed with brine and dried over anhydrous Na_2SO_4. The solvent was evaporated, and the remaining crude product was purified by column chromatography to give desired compounds **7a–c**.

2.4.2 General procedure for the synthesis of compounds 8a, 8b, 8c. In a 100 mL round bottom flask, compound **7a–c** (0.215 mmol) was taken in dichloroethane (15 mL) followed by the addition of anhydrous DMF (0.237 mmol) at room temperature. Then the reaction solution was cooled to 0 °C, and $POCl_3$ (0.86 mmol) was added dropwise. The reaction mixture was allowed to warm to room temperature and refluxed overnight, and waked up with saturated sodium acetate solution. The

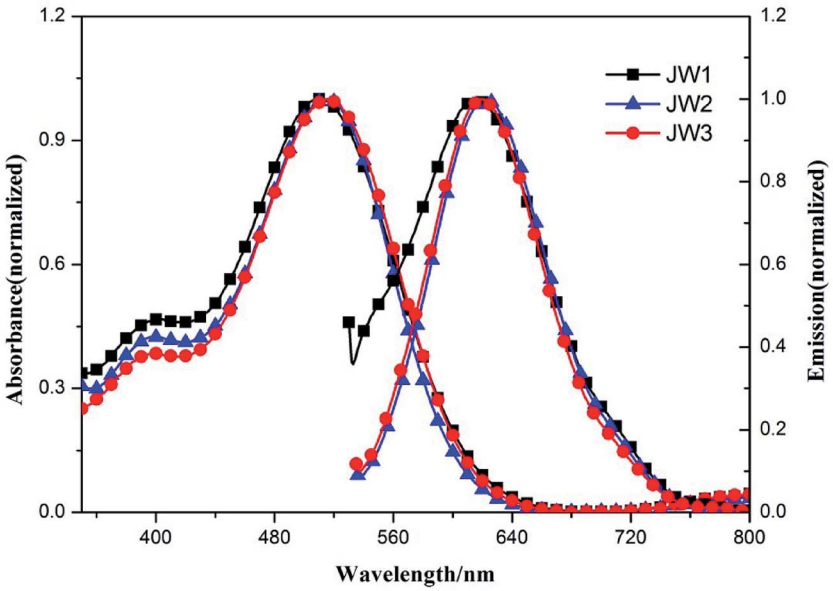

(a)

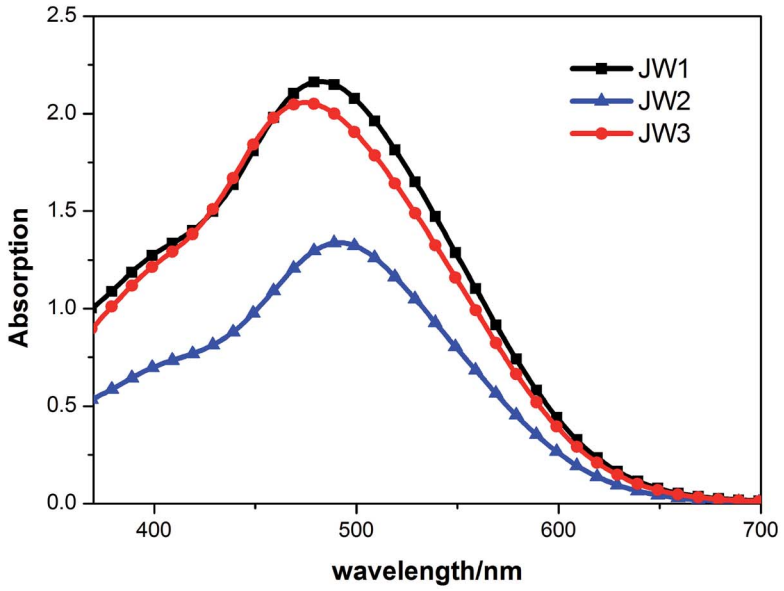

(b)

Fig. 2 The absorption and emission spectra of **JW1**, **JW2** and **JW3** (a) in dichloromethane and (b) on TiO_2 films.

Table 1 Photophysical and electrochemical data of JW1, JW2 and JW3

Dye	$\lambda_{max,sol}$ [a] (nm)	ε (10^4 M^{-1} cm^{-1})	$\lambda_{max,film}$ [b] (nm)	λ_{int} [c] (nm)	Adsorbed dye[d] 10^{-6} mol cm^{-2}	HOMO[e]/*vs.* NHE (eV)	LUMO[f]/*vs.* NHE (eV)	E_{0-0} [c] (eV)
JW1	510	3.23	482	614	4.6	1.014	−1.186	2.20
JW2	515	4.63	490	622	1.6	0.996	−1.174	2.17
JW3	516	3.48	472	620	3.1	0.914	−1.246	2.16

[a] The maximum absorption wavelength of UV-vis spectra measured in dichloromethane. [b] The maximum absorption wavelength of UV-vis spectra measured on TiO_2. [c] λ_{int} is the intersections of normalized absorption and emission spectra in dichloromethane; E_{0-0} values were estimated from $E_{0-0} = 1240/\lambda_{int}$. [d] The adsorbed amount of dye on the TiO_2 surface. [e] HOMO (*vs.* NHE) were measured in acetonitrile and calibrated with ferrocene (0.63 V *vs.* NHE). [f] LUMO (*vs.* NHE) were estimated from calculated from LUMO = HOMO–E_{0-0}.

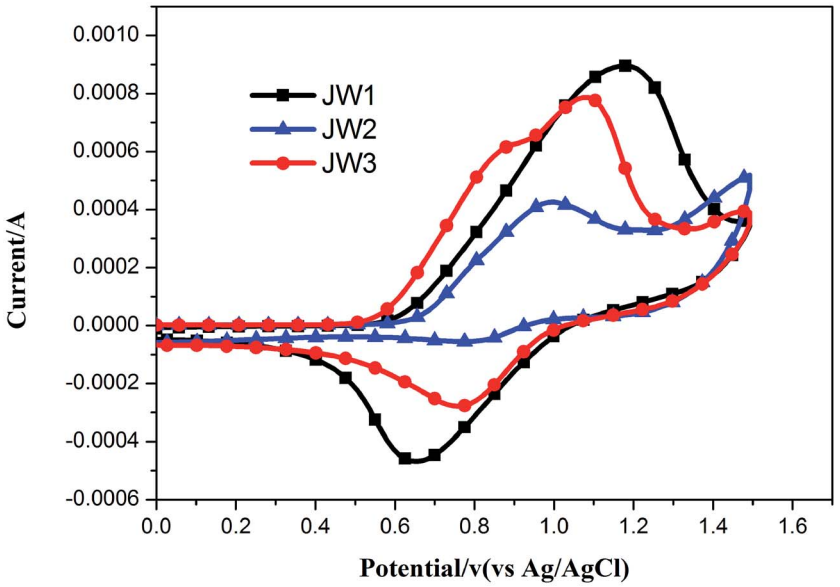

(a)

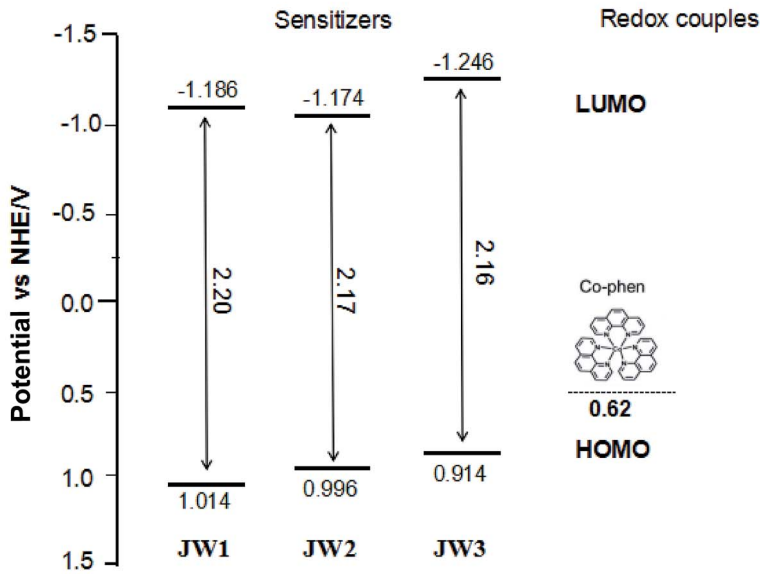

(b)

Fig. 3 (a) Cyclic voltammograms of JW1, JW2 and JW3 measured in acetonitrile solutions; (b) energy levels of dyes and redox couples.

product was extracted with dichloromethane, washed with water and brine, and then dried over anhydrous Na_2SO_4.

2.4.3 General procedure for the synthesis of compounds JW1, JW2 and JW3. To a stirred solution of compound **8a–c** (0.11 mmol) and cyanoacetic acid (0.164 mmol, 14 mg) in acetonitrile (6 mL) was added chloroform (3 mL) and piperidine (0.33 mmol, 28 mg). The reaction mixture was refluxed for 8 h. Then additional cyanoacetic acid (0.164 mmol) and piperidine (0.33 mmol, 28 mg) were added. The mixture was refluxed continuously for 8 hours and then acidified with 1 M hydrochloric acid aqueous solution (15 mL). The crude product was extracted into CH_2Cl_2, washed with water and brine, and then dried over anhydrous Na_2SO_4. After that the solvent was evaporated, and the remaining crude product was purified by column chromatography to give desired compounds **JW1**, **JW2** and **JW3**.

3. Results and discussion

The synthetic routes for **JW1**, **JW2** and **JW3** were shown in Scheme 1. The aldehyde intermediates (**6a–c**) play a key role in obtaining the target dye molecules. All intermediates and final products are purified and characterized by NMR spectra. The spectroscopic and electrochemical properties of **JW1**, **JW2** and **JW3** were tested and analyzed, respectively.

3.1. Absorption spectra

Absorption and emission spectra of **JW1**, **JW2** and **JW3** were studied by UV-vis spectroscopy and fluorescence spectroscopy, and the optical band gaps (E_{0-0}) of the three dyes are calculated from the intersections of normalized absorption and emission spectra. Fig. 2(a) shows the normalized absorption and emission spectra of **JW1**, **JW2** and **JW3** in dichloromethane. The maximum absorption wavelength in dichloromethane of **JW1**, **JW2** and **JW3** show little difference, which are 510 nm, 515 nm and 516 nm, respectively. This suggests the bulky groups are not key point for increasing the light response, while the basic D–π–A skeleton is a more important factor for their absorption ability. Subsequently, the molar extinction coefficients of the dye solution with the concentration of 1.5×10^{-5} M were measured. As listed in Table 1, the corresponding molar extinction coefficients of **JW1**, **JW2** and **JW3** in dichloromethane are 3.23×10^4 M^{-1} cm^{-1}, 4.63×10^4 M^{-1} cm^{-1} and 3.48×10^4 M^{-1} cm^{-1}, respectively. **JW2** shows the highest molar extinction among the three dyes in solution. The intersections of normalized absorption and emission spectra of **JW1**, **JW2** and **JW3** are at 614 nm, 622 nm and 620 nm, respectively. Thus, the E_{0-0} values of **JW1**, **JW2** and **JW3** are 2.20 eV, 2.17 eV, and 2.16 eV, separately.[37] The multi-alkyl groups of **JW2** and **JW3** relatively reduce the E_{0-0} value as compared to **JW1**. The absorption spectra of the studied dyes anchored on mesoporous TiO_2 were also investigated, as shown in Fig. 2(b). Three dyes absorbing on TiO_2 display obvious absorption extended to 700 nm. While the weaker absorbance of **JW2** on TiO_2 due to its larger molecular size than **JW1** and **JW3** causing a decrease of absorbed amount on TiO_2 per square centimeter. The absorbed amounts of **JW1**, **JW2** and **JW3** on 3 μm-thick TiO_2 films are 4.6×10^{-6} mol cm^{-2}, 1.6×10^{-6} mol cm^{-2} and 3.1×10^{-6} mol cm^{-2}, respectively. The spectroscopic data are summarized in Table 1.

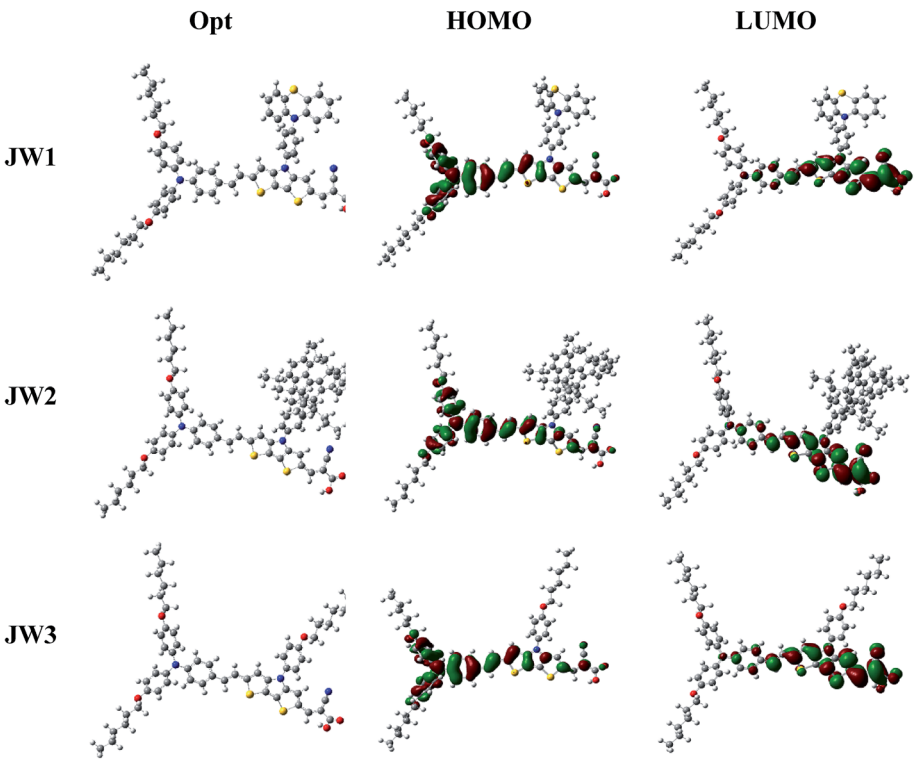

Fig. 4 The Frontier molecular orbital distributions of JW1, JW2 and JW3 optimized by DFT calculations at the B3LYP/6-31G level.

3.2. Electrochemical properties and theoretical calculations

The structure effect on energy levels has a great impact on getting a suitable drive force for dye regeneration in DCCSs. Cyclic voltammograms (CV) was conducted to determine the accurate highest occupied molecular orbital (HOMO) and lowest unoccupied molecular orbital (LUMO) levels of **JW1**, **JW2** and **JW3**. The CV curves of three dyes in acetonitrile are shown in Fig. 3(a). The electrochemical data and related calculation methods are given in Table 1. The HOMO levels of **JW1**, **JW2** and **JW3** corresponding to the first oxidation potentials was 1.104 eV, 0.996 eV and 0.914 eV (*vs.* NHE), respectively. The LUMO levels of **JW1**, **JW2** and **JW3** are −1.186 eV, −1.174 eV and −1.246 eV (*vs.* NHE), respectively. The LUMO levels of the three dyes are more negative than the conduction band (CB) of the

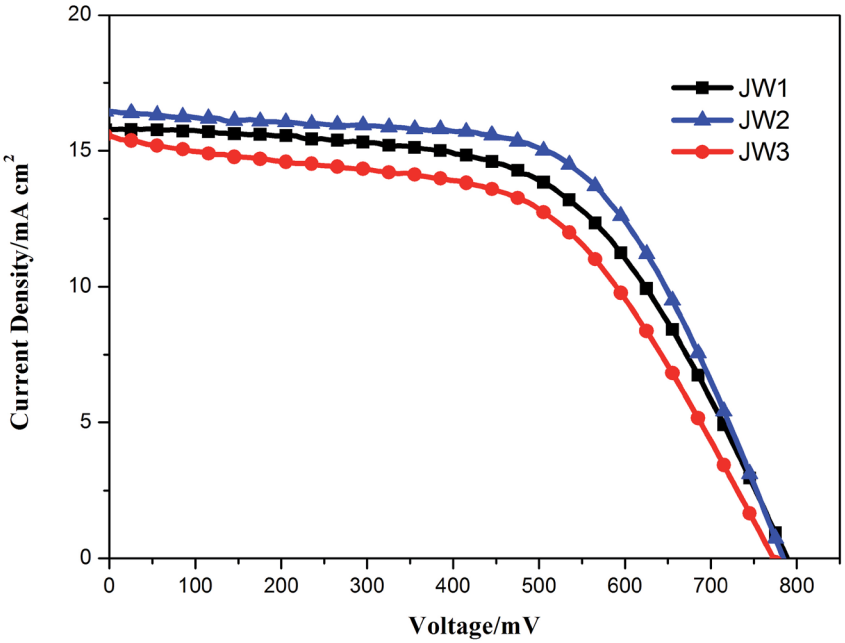

(a)

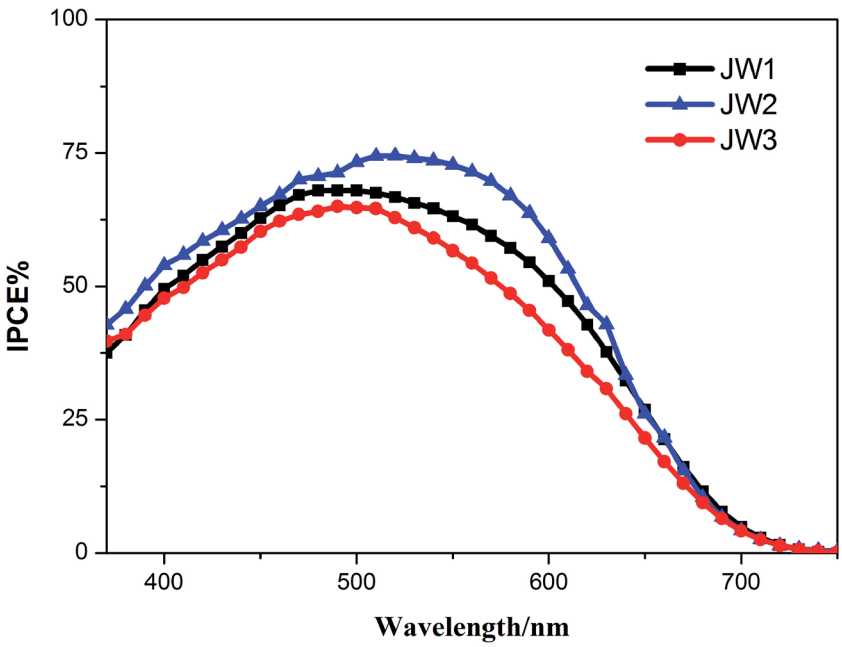

(b)

Fig. 5 (a) *J*–*V* curves and (b) IPCE spectra of DSSCs based on **JW1**, **JW2** and **JW3**.

Table 2 Photovoltaic parameters of the DSSCs based on **JW1**, **JW2** and **JW3**

Dye	J_{sc}/MA cm^2	V_{oc}/mV	FF	PCE%
JW1	15.79	788	0.57	7.09
JW2	16.45	784	0.61	7.87
JW3	15.57	773	0.54	6.50

TiO_2 electrode (−0.5 V *vs.* NHE), making it easily for electron injection into the CB of TiO_2. Based on the spectroscopic and electrochemical data, the energy-level diagram of **JW1**, **JW2** and **JW3** are depicted in Fig. 3(b). The energy levels of the studied dyes are well matched with the CB of TiO_2 and the redox energy of the selected Co-phen electrolyte.

To gain insight into the electronic properties and geometries of **JW1**, **JW2** and **JW3**, quantum chemical calculations were

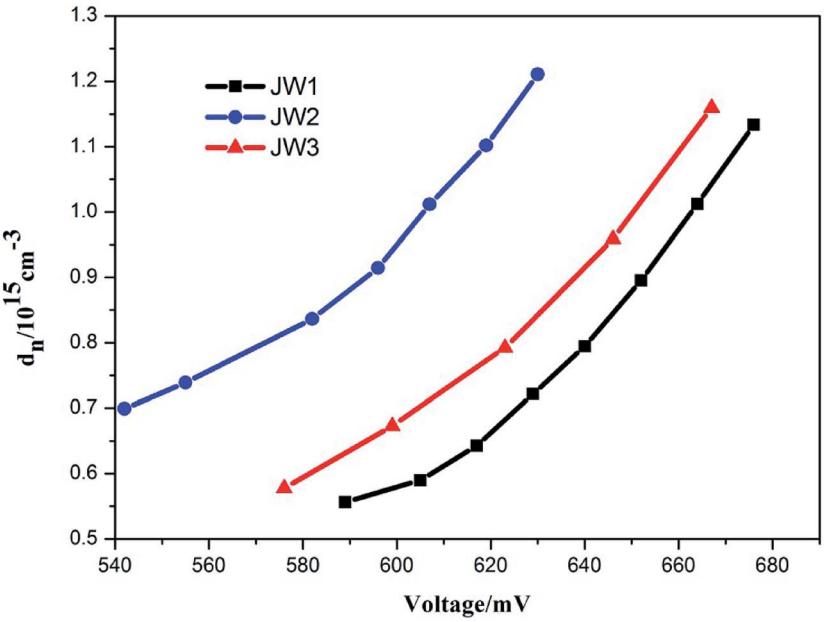

(a)

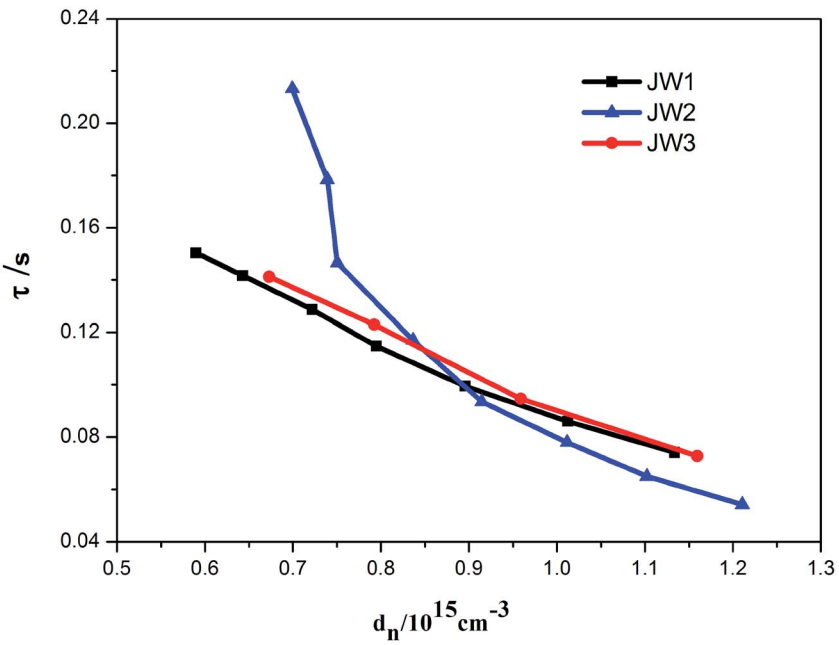

(b)

Fig. 6 (a) Charge density as the open circuit and (b) electron lifetime as the charge density for DSSCs based on the dyes **JW1**, **JW2** and **JW3**.

performed. Their geometric structures were optimized on the basis of density functional theory (DFT) at the B3LYP/6-31G level. All structural optimization and energy calculations were performed using the GAUSSIAN 09 program. The optimized structures and the Frontier orbitals of molecules of **JW1**, **JW2** and **JW3** are shown in Fig. 4. The HOMOs of **JW1**, **JW2** and **JW3** are extended over the whole backbone of dye molecules, and the LUMOs are effectively transferred from the arylamine donor to the acceptor part unit *via* the DTP spacer. The optimized structures of **JW1**, **JW2** and **JW3** are shown in Fig. S1 and S2,† and the corresponding data on the representative dihedral angles and bond lengths are listed in Table S1 (ESI).† In Fig. S2,† the dihedral angles between DTP and its chains for **JW1**, **JW2** and **JW3** are 126.9°, 125.9° and 126.9°, respectively. The DTP spacer on **JW2** exhibits a little more twisted structure due to the larger size of truxene unit. Based on the photovoltaic performances discussed on Section 3.4, the little twisted change on **JW2** has a positive effect on reducing charge recombination on interfaces in DSSCs.

3.3. Photovoltaic performances of DSSCs

DSSCs based on **JW1**, **JW2** and **JW3** were fabricated with Co-phen electrolyte. The photovoltaic performances of devices based on **JW1**, **JW2** and **JW3** were investigated by photocurrent–voltage (*J*–*V*) measurements. The *J*–*V* curves are shown in Fig. 5(a), and the corresponding photovoltaic parameters are listed in Table 2. In Fig. 5(a), devices based on **JW1**, **JW2** and **JW3** show a PCE of 7.09%, 7.87% and 6.50%, respectively. **JW2**-based DSSCs exhibit the highest PCE, yielding a J_{sc} of 16.45 mA cm^2, a V_{oc} of 784 mV and a FF of 0.61. As shown in Fig. 3(b), the suitable HOMO–LUMO energy gap of **JW2** can both strengthens electron injection from dye to TiO_2 and reduces driving force for the regeneration of oxidized dye among the three dyes, making the corresponding device based on **JW2** display the highest J_{sc} value. In Fig. 5(b), the corresponding incident photon-to-current conversion efficiency (IPCE) spectra of DSSCs fabricated by **JW1**, **JW2** and **JW3** were recorded. Correspondingly, IPCE values of **JW1** and **JW2**-based DSSCs are higher than that of **JW3**-based DSSCs. As listed in Table 1, the absorbed **JW1**, **JW2** and **JW3** on TiO_2 are 4.6×10^{-6} mol cm^{-2}, 1.6×10^{-6} mol cm^{-2} and 3.1×10^{-6} mol cm^{-2}, respectively. Although the amount of **JW2** absorbed on TiO_2 is the least among the three dyes due to the large size of truxene unit, **JW2**-based cells achieved the best performance.

In order to further study the relationship between dye structures and device performances, the charge density (d_n) at open circuit and the electron lifetime (τ) as a function of charge density were measured by controlled intensity modulated photovoltage spectroscopy (IMVS).[38–40] The results indicate that the introduction of 10-phenyl-10*H*-phenothiazine and truxene onto DTP spacers of **JW1** and **JW2** is benefit to enhance the photovoltaic performances of DSSCs by more efficiently reduce electron recombination, as compared to the introduction of 4-hexyloxyphenyl onto DTP spacers of **JW3**. As shown in Fig. 6(a), TiO_2 grafted with **JW1**, **JW2** and **JW3** displays an increased V_{oc} value in the order of **JW2** < **JW3** < **JW1** at a fixed d_n, indicating the introduction of bulky groups on DTP has an obvious impact on the CB shift of TiO_2.[27,41] TiO_2 grafted with **JW2** caused a downward CB shift of TiO_2 compared to **JW1** and **JW3**. However, the LUMO level of **JW2** is low enough to make sure efficient electron injection from **JW2** to TiO_2. Therefore, the different bulky groups feasibly regulate HOMO–LUMO energy gap of the studied sensitizers, the suitable energy levels have a positive effect on fabricating highly-efficient DSSCs. As shown in Fig. 6(b), the τ value of **JW2** exhibits a certain increase than those of devices based on **JW1** and **JW3**, which may be more favorable to reduce charge recombination in the device. Truxene is a good building block for the modification on π-spacers of sensitizers in DSSCs.

4. Conclusions

New D–π–A organic dyes with dithieno[3,2-*b*:2′,3′-*d*]pyrrole (DTP) π-spacers (**JW1**, **JW2** and **JW3**) were synthesized for fabricating efficient DSSCs in Co-phen based electrolyte. Different bulky groups were introduced onto the DTP unit, and the structure–efficiency relationship was investigated by theoretical calculations, spectroscopic, electrochemical and photovoltaic measurements. The three dyes display strong absorption at the range of 400–700 nm both in solution and on TiO_2 film. CV measurements show that **JW2** incorporating DTP with truxene shows modest energy levels for reducing drive force for electron injection and dye regeneration. Based on *J*–*V* results, DSSCs fabricated by **JW2** exhibit the highest PCE of 7.87%, and that of cells based on **JW1** and **JW3** are 7.09% and 6.50%. Devices based on **JW1** and **JW2** with lager bulky units yield higher J_{sc} and V_{oc} values than that based on **JW3**. IMVS results indicate the three dyes have an obvious influence on the CB shift of TiO_2 *via* the introduction of different substitutes on DTP π-spacer, and differs the inhibition ability of charge recombination in device. Therefore, suitable design of dye molecules has a great effect on improve the photovoltaic performances of DSSCs.

Conflicts of interest

There are no conflicts to declare.

Acknowledgements

This work was supported by the National Natural Science Foundation of China (21376179, 21506164).

References

1 B. O'regan and M. Grätzel, A low-cost, high-efficiency solar cell based on dye-sensitized colloidal TiO_2 films, *Nature*, 1991, **353**, 737–740.
2 Y. Z. Wu, W. H. Zhu, S. M. Zakeeruddin and M. Grätzel, Insight into D–A–π–A structured sensitizers: a promising route to highly efficient and stable dye-eensitized solar cells, *ACS Appl. Mater. Interfaces*, 2015, **7**, 9307–9318.

3 L. Wei, Y. Na, Y. L. Yang, R. Q. Fan, P. Wang and L. Li, Efficiency of ruthenium dye sensitized solar cells enhanced by 2,6-bis[1-(phenylimino)ethyl]pyridine as a co-sensitizer containing methyl substituents on its phenyl rings, *Phys. Chem. Chem. Phys.*, 2015, **17**, 1273–1280.

4 H. Ozawa, T. Sugiura, T. Kuroda, K. Nozawa and H. Arakawa, Highly efficient dye-sensitized solar cells based on a ruthenium sensitizer bearing a hexylthiophene modified terpyridine ligand, *J. Mater. Chem. A*, 2016, **4**, 1762–1770.

5 H. Ozawa, S. Honda, D. Katano, T. Sugiura and H. Arakawa, Novel ruthenium sensitizers with a dianionic tridentate ligand for dye-sensitized solar cells: the relationship between the solar cell performances and the electron-withdrawing ability of substituents on the ligand, *Dalton Trans.*, 2014, **43**, 8026–8036.

6 H. Cheema, A. Islam, L. Han and A. El-Shafei, Monodentate pyrazole as a replacement of labile NCS for Ru(II) photosensitizers: Minimum electron injection free energy for dye-sensitized solar cells, *Dyes Pigm.*, 2015, **120**, 93–98.

7 H. Cheema, L. Ogbose and A. El-Shafe, Structure–property relationships: steric effect in ancillary ligand and how it influences photocurrent and photovoltage in dye-sensitized solar cells, *Dyes Pigm.*, 2015, **113**, 151–159.

8 E. Schönhofer, B. Bozic-Weber, C. J. Martin, E. C. Constable, C. E. Housecroft and J. A. Zampese, Surfaces-as-ligands, surfaces-as-complexes, strategies for copper(I) dye-sensitized solar cells, *Dyes Pigments*, 2015, **115**, 154–165.

9 M. Liang and J. Chen, Arylamine organic dyes for dye-sensitized solar cells, *Chem. Soc. Rev.*, 2013, **42**, 3453–3488.

10 C. P. Lee, R. Y. Lin, L. Y. Lin, C. T. Li, T. C. Chu, S. S. Sun, J. T. Lin and K. C. Ho, Recent progress in organic sensitizers for dye-sensitized solar cells, *RSC Adv.*, 2015, **5**, 23810–23825.

11 S. Ahmad, E. Guillén, L. Kavan, M. Grätzel and M. K. Nazeeruddin, Metal free sensitizer and catalyst for dye sensitized solar cells, *Energy Environ. Sci.*, 2013, **6**, 3439–3466.

12 A. L. Capodilupo, L. D. Marco, G. A. Corrente, R. Giannuzzi, E. Fabiano, A. Cardone, G. Gigl and G. Ciccarella, Synthesis and characterization of a new series of dibenzofulvene based organic dyes for DSSCs, *Dyes Pigm.*, 2016, **130**, 79–89.

13 M. Grishina, O. Bol'shakov, A. Potemkin and V. Potemkin, Benzo[1,2,5]thiadiazole dyes: Spectral and electrochemical properties and their relation to the photovoltaic characteristics of the dye-sensitized solar cells, *Dyes Pigm.*, 2017, **144**, 80–93.

14 C. Maglione, A. Carella, C. Carbonara, R. Centore, S. Fusco, A. Velardo, A. Peluso, D. Colonna, A. Lanuti and A. D. Carlo, Novel pyran based dyes for application in dye sensitized solar cells, *Dyes Pigm.*, 2016, **133**, 395–405.

15 K. Kakiage, Y. Aoyama, T. Yano, T. Otsuka, T. Kyomen and M. Unno, An achievement of over 12 percent efficiency in an organic dye-sensitized solar cel, *Chem. Commun.*, 2014, **50**, 6379–6381.

16 K. Kakiage, Y. Aoyama, T. Yano, K. Oya, J. I. Fujisawa and M. Hanaya, Highly-efficient dye-sensitized solar cells with collaborative sensitization by silyl-anchor and carboxy-anchor dyes, *Chem. Commun.*, 2015, **51**, 15894–15897.

17 W. H. Zhu, Y. Wu, S. Wang, W. Li, X. Li, J. Chen, Z. Wang and H. Tian, Organic D–A–π–A solar cell sensitizers with improved stablility and soectral response, *Adv. Funct. Mater.*, 2011, **1**, 756–763.

18 M. Freitag, J. Teuscher, Y. Saygili, X. Zhang, F. Giordano, P. Liska, J. Hua, S. M. Zakeeruddin, J. E. Moser, M. Grätzel and A. Hagfeldt, Dye-sensitized solar cells for efficient power generation under ambient lighting, *Nat. Photonics*, 2017, **11**, 372–378.

19 T. Hao, Y. Saygili, J. Cong, A. Eriksson, W. Yang, J. Zhang, E. Polanski, K. Nonomura, M. Z. ZakeeruddinShaik, M. Grätzel, A. Hagfeldt and G. Boschloo, Novel blue organic dye for dye-sensitized solar cells achieving high efficiency in cobalt-based electrolytes and by co-sensitization, *ACS Appl. Mater. Interfaces*, 2016, **8**, 32797–32804.

20 C. Y. Lo, D. Kumar, S. H. Chou, C. H. Chen, C. H. Tsai, S. H. Liu, P. T. Chou and K. T. Wong, Highly twisted dianchoring D–π–A sensitizers for efficient dye-sensitized solar cells, *ACS Appl. Mater. Interfaces*, 2016, **8**, 27832–27842.

21 P. Dai, H. Dong, M. Liang, H. Cheng, Z. Sun and S. Xue, Understanding the role of electron donor in truxene dye sensitized solar cells with cobalt electrolytes, *ACS Sustainable Chem. Eng.*, 2017, **5**, 97–104.

22 Y. K. Eom, J. Y. Hong, J. Kim and H. K. Kim, Triphenylamine-based organic sensitizers with π-spacer structural engineering for dye-sensitized solar cells: synthesis, theoretical calculations, molecular spectroscopy and structure-property-performance relationships, *Dyes Pigm.*, 2017, **136**, 496–504.

23 S. M. Fernandes, M. Mesquit, L. Andrade, A. Mendes and M. Raposo, Synthesis and characterization of novel thieno[3,2-*b*]thiophene based metal-free organic dyes with different heteroaromatic donor moieties as sensitizers for dye-sensitized solar cells, *Dyes Pigm.*, 2017, **1**, 46–53.

24 A. Yella, H. B. Robin, B. F. E. Curchod, N. A. Astani, J. Teuscher, L. E. Polander, S. Mathew, J. E. Moser, I. Tavernelli, U. Rothlisberger, M. Grätzel, M. K. Nazeeruddin and J. Frey, Molecular engineering of a fluorene donor for dye-sensitized solar cells, *Chem. Mater.*, 2013, **25**, 2733–2739.

25 P. Gao, H. N. Tsao, M. Grätzel and M. K. Nazeeruddin, Fine-tuning the electronic structure of organic dyes for dye-sensitized solar cell, *Org. Lett.*, 2012, **14**, 4330–4333.

26 X. Zhang, Y. Xu, F. Giordano, M. Schreier, N. Pellet, Y. Hu, C. Yi, N. Robertson, J. Hua, S. M. Zakeeruddin, H. Tian and M. Grätzel, Molecular engineering of potent sensitizers for very efficient light harvesting in thin-film solid-state dye-sensitized solar cells, *J. Am. Chem. Soc.*, 2016, **138**, 10742–10745.

27 Z. Wang, M. Liang, H. J. Yu, Y. Zhang, L. Wang, Z. Sun and S. Xue, Influence of the N-heterocycle substituent of the dithieno[3,2-*b*:2′,3′-*d*]pyrrole (DTP) spacer as well as sensitizer adsorption time on the photovoltaic properties of arylamine organic dyes, *J. Mater. Chem. A*, 2013, **1**, 11809–11819.

28 Y. Xie, W. Wu, H. Zhu, J. Liu, W. Zhang, H. Tian and W. H. Zhu, Unprecedentedly targeted customization of

molecular energy levels with auxiliary-groups in organic solar cell sensitizers, *Chem. Sci.*, 2016, **7**, 544–549.

29 F. S. Li, Y. Chen, X. P. Zong, W. H. Qiao, H. Y. Fan, M. Liang and S. Xue, New benzothiadiazole-based dyes incorporating dithieno[3,2-*b*:2′,3′-*d*]pyrrole (DTP) π-linker for dye-sensitized solar cells with different electrolytes, *J. Power Sources*, 2016, **332**, 345–354.

30 H. Dong, M. Liang, C. Zhang, Y. Wu, Z. Sun and S. Xue, Twisted fused-ring thiophene organic dye-sensitized solar cells, *J. Phys. Chem. C*, 2016, **120**, 22822–22830.

31 Z. Wang, M. Liang, Y. Hao, Y. Zhang, L. Wang, Z. Sun and S. Xue, Influence of the N-heterocycle substituent of the dithieno[3,2-*b*:2′,3′-*d*]pyrrole (DTP) spacer as well as sensitizer adsorption time on the photovoltaic properties of arylamine organic dyes, *J Mater. Chem. A*, 2013, **1**, 11809–11819.

32 L. E. Polander, A. Yella, J. Teuscher, R. Humphry-Bake, B. Curchod, N. A. Astani, P. Gao, J. E. Moser, I. Tavernelli, U. Rothlisberger, M. Grätzel, M. K. Nazeeruddin and J. Frey, Unravelling the potential for dithienopyrrole sensitizers in dye-sensitized solar cells, *Chem. Mater.*, 2013, **25**, 2642–2648.

33 D. H. Lee, M. J. Lee, H. M. Song, B. J. Song, K. D. Seo, M. Pastore, C. Anselmi, F. D. Angelis and M. K. Nazeeruddin, Organic dyes incorporating low-band-gap chromophores based on π-extended benzothiadiazole for dye-sensitized solar cell, *Dyes Pigm.*, 2011, **91**, 192–198.

34 T. Ganesh, H. M. Nguyen, R. S. Mane, N. Kim, D. V. Shinde and S. S. Bhande, Promising ZnO-based DSSC performance using HMP molecular dyes of high extinction coefficients, *Dalton Trans.*, 2014, **43**, 11305–11308.

35 J. Liu, D. Zhou, M. Xu, X. Jing and P. Wang, The structure–property relationship of organic dyes in mesoscopic titania solar cells: only one double-bond difference, *Energy Environ. Sci.*, 2011, **4**, 3545–3551.

36 W. H. Nguyen, C. D. Bailie, J. Burschka, T. Moehl, M. Grätzel and M. D. Mcgehee, Molecular engineering of organic dyes for improved recombination lifetime in solid-state dye-sensitized solar cells, *Chem. Mater.*, 2013, **25**, 1519–1525.

37 M. Grishina, O. Bol'shakov, A. Potemkin and V. Potemkin, Benzo[1,2,5]thiadiazole dyes: Spectral and electrochemical properties and their relation to the photovoltaic characteristics of the dye-sensitized solar cells, *Dyes Pigm.*, 2017, **144**, 80–93.

38 Z. S. Huang, L. H. Feng, X. F. Zang, Z. Iqbal, H. Zeng and D. B. Kuang, Dithienopyrrolobenzothiadiazole-based organic dyes for efficient dye-sensitized solar cells, *J. Mater. Chem. A*, 2014, **2**, 15365–15376.

39 J. H. Lee, C. H. Park, J. P. Jung and J. H. Kim, Worm-like mesoporous TiO_2 thin films templated using comb copolymer for dye-sensitized solar cells with polymer electrolyte, *J. Power Sources*, 2015, **298**, 14–22.

40 Y. Q. Wang, J. Lua, J. Yina, G. Lü, Y. M. Cui, S. S. Wang, S. Y. Deng, D. Shan, H. L. Tao and Y. M. Sun, Influence of 4-*tert*-butylpyridine/guanidinium thiocyanate co-additives on band edge shift and recombination of dye-sensitized solar cells: experimental and theoretical aspects, *Electrochim. Acta*, 2015, **185**, 69–75.

41 X. L. Hao, M. Liang, X. B. Cheng, X. Q. Pian, Z. Sun and S. Xue, Organic dyes incorporating the benzo[1,2-*b*:4,5-*b*′] dithiophene moiety for efficient dye-sensitized solar cells, *Org. Lett.*, 2011, **13**, 5424–5427.